Conference Paper Manuscript
APT#: 123602

Benchmark Simulations of the Thermal-Hydraulic Responses during EBR-II Inherent Safety Tests using SAM

prepared by
Rui Hu and Tyler Sumner

Nuclear Engineering Division
Argonne National Laboratory
9700 South Cass Avenue, Bldg. 208
Argonne, IL 60439-4854

The submitted manuscript has been created by UChicago Argonne, LLC, Operator of Argonne National Laboratory ("Argonne"). Argonne, a U.S. Department of Energy Office of Science laboratory, is operated under Contract No. DE-AC02-06CH11357. The U.S. Government retains for itself, and others acting on its behalf, a paid-up nonexclusive, irrevocable worldwide license in said article to reproduce, prepare derivative works, distribute copies to the public, and perform publicly and display publicly, by or on behalf of the Government. The Department of Energy will provide public access to these results of federally sponsored research in accordance with the DOE Public Access Plan.
http://energy.gov/downloads/doe-public-accessplan

2016 International Congress on Advances in Nuclear Power Plants
ICAPP'16
April 17-20, 2016
San Francisco, CA
USA

About Argonne National Laboratory
Argonne is a U.S. Department of Energy laboratory managed by UChicago Argonne, LLC under contract DE-AC02-06CH11357. The Laboratory's main facility is outside Chicago, at 9700 South Cass Avenue, Argonne, Illinois 60439. For information about Argonne and its pioneering science and technology programs, see www.anl.gov.

Disclaimer
This manuscript was prepared as an account of work sponsored by an agency of the United States Government. Neither the United States Government nor any agency thereof, nor UChicago Argonne, LLC, nor any of their employees or officers, makes any warranty, express or implied, or assumes any legal liability or responsibility for the accuracy, completeness, or usefulness of any information, apparatus, product, or process disclosed, or represents that its use would not infringe privately owned rights. Reference herein to any specific commercial product, process, or service by trade name, trademark, manufacturer, or otherwise, does not necessarily constitute or imply its endorsement, recommendation, or favoring by the United States Government or any agency thereof. The views and opinions of document authors expressed herein do not necessarily state or reflect those of the United States Government or any agency thereof, Argonne National Laboratory, or UChicago Argonne, LLC.

BENCHMARK SIMULATIONS OF THE THERMAL-HYDRAULIC RESPONSES DURING EBR-II INHERENT SAFETY TESTS USING SAM

Rui Hu and Tyler Sumner

Argonne National Laboratory, 9700 S. Cass Avenue, Argonne, IL 60439, USA, rhu@anl.gov

An advanced system analysis tool SAM is being developed for fast-running, improved-fidelity, and whole-plant transient analyses at Argonne National Laboratory under DOE-NE's Nuclear Energy Advanced Modeling and Simulation (NEAMS) program. As an important part of code development, companion validation activities are being conducted to ensure the performance and validity of the SAM code. This paper presents the benchmark simulations of two EBR-II tests, SHRT-45R and BOP-302R, whose data are available through the support of DOE-NE's Advanced Reactor Technology (ART) program. The code predictions of major primary coolant system parameter are compared with the test results. Additionally, the SAS4A/SASSYS-1 code simulation results are also included for a code-to-code comparison.

I. INTRODUCTION

An advanced system analysis tool SAM (Ref. [1]) is being developed at Argonne National Laboratory under the DOE-NE's Nuclear Energy Advanced Modeling and Simulation (NEAMS) program. The goal of the SAM development is to provide fast-running, improved-fidelity whole-plant transient analyses capabilities. SAM utilizes an object-oriented application framework MOOSE (Ref. [2]), and its underlying meshing and finite-element library libMesh (Ref. [3]), as well as linear and non-linear solvers PETSc (Ref. [4]), to leverage modern advanced software environments and numerical methods. It incorporates advances in physical and empirical models and seeks closure models based on information from high-fidelity simulations and experiments. Additionally, coupling interfaces have been developed to allow for convenient integration with other advanced or conventional simulation tools for multi-scale and multi-physics modeling capabilities.

Extensive experimental studies of inherent safety characteristics of Liquid-Metal-cooled Fast Reactor (LMFR) systems have been conducted in the Experimental Breeder Reactor II (EBR-II, Ref. [5]). These tests demonstrated its capabilities of heat removal without the aid of active safety systems, as well as the capabilities to mitigate a reduction in core cooling flow or heat rejection to the balance of plant (BOP) without the aid of active control or protection systems. Another objective of the program was to provide data for computer code validation so that the results of the testing can be extrapolated and applied to other LMFR designs. To support this objective an extensive data set was recorded for each test by the plant data acquisition system. Through an ongoing effort under DOE-NE's Advanced Reactor Technology (ART) program, some of the EBR-II test data are recovered and organized into electronic databases.

As an important part of code development, validation activities are being conducted to assure the performance and validity of the SAM code. This paper presents the benchmark simulations of two EBR-II tests, an unprotected loss of forced cooling flow test (SHRT-45R) and an unprotected loss of all heat rejection test (BOP-302R). The code predictions of major primary coolant system parameter are compared with the test results. Additionally, the SAS4A/SASSYS-1 (Ref. [6]) code simulation results are also included for a code-to-code comparison.

II. SAM OVERVIEW

SAM is being developed as a system-level modeling and simulation tool with improved accuracy while remaining computationally efficient. It is aimed at solving the tightly-coupled physical phenomena including fission reaction, heat transfer, fluid dynamics, and thermal-mechanical response in SFR structures, systems and components in a fully-coupled fashion. Reduced-order modeling approaches are used to facilitate rapid turn-around for design and safety optimization studies. As a new code development, the initial effort focused on developing modeling and simulation capabilities of the heat transfer and single-phase fluid dynamics responses in the SFR systems. The details of the tool development and its status can be found in Ref. [1].

SAM employs a one-dimensional transient model for single-phase incompressible but thermally expandable flow. The governing equations consist of the continuity, momentum, and energy equations. A three dimensional module is also under development to model the multi-dimensional flow and thermal stratification in the upper plenum or the cold pool in an SFR reactor vessel. Additionally, a subchannel module will be developed for more-detailed fuel assembly modeling. The details of the one-dimensional single-phase flow model for incompressible thermally expandable flow and the stabilization schemes can be found in Ref. [7].

Heat structures in SAM model the heat conduction inside the solids and permit the modeling of convective heat transfer at the interfaces between solid and fluid components. It can represent one-dimensional or two-dimensional heat conduction in Cartesian or cylindrical

coordinates. Temperature-dependent thermal conductivities and volumetric heat capacities can be provided in tabular or functional form either from built-in or user-supplied data. The modeling capabilities of heat structures can be used to predict the temperature distributions in solid components such as fuel pins or plates, heat exchanger tubes, and pipe and vessel walls, as well as to calculate the heat flux conditions for fluid components. A flexible conjugate heat transfer modeling capability is implemented in SAM, and the details can be found in Ref. [8].

The Jacobian-Free Newton Krylov (JFNK) solution method is used to solve the equation system. The JFNK method is a multi-level approach, the outer Newton iterations (nonlinear solver) and inner Krylov subspace methods (linear solver), in solving large nonlinear systems. One great feature of JFNK is that all the unknowns are solved simultaneously in a fully coupled fashion. This solution scheme avoids the errors from operator splitting and is especially suitable for conjugate heat transfer problems in which the heat conduction in the solid is tightly coupled with the fluid flow.

The physics modeling and mesh generation of individual reactor components are encapsulated as Component classes in SAM. A set of components has been developed based on the FEM fluid model and heat conduction model, including: (1) basic fluid and solid geometric components; (2) 0-D components for setting boundary conditions; (3) 0-D components for connecting 1-D fluid components; (4) assembly components by combining the basic geometric components and the 0-D connecting components; and (5) non-geometric components for physics integration. The transient simulation capabilities of typical SFR accidents have been demonstrated in a number of reactor transient simulations[1].

III. TEST DESCRIPTIONS

The EBR-II plant was a 62.5 MWth metallic fueled sodium fast reactor designed and operated between 1964 and 1994 by Argonne National Laboratory. During its operation, EBR-II was used for experiments designed to demonstrate the feasibility of passive safety in liquid metal reactors (LMR). The Shutdown Heat Removal Test program was carried out in EBR-II between 1984 and 1986. The objectives of the program were to support the U.S. advanced LMR program, provide test data for validation of computer codes, and demonstrate passive reactor shutdown and decay heat removal in response to protected and unprotected transients.

Argonne has performed analyses of SHRT-17 and SHRT-45R, the most severe protected and unprotected loss of flow tests, using SAS4A/SASSYS-1 under an ongoing four-year International Atomic Energy Agency (IAEA) coordinated research project[9,10]. The benchmark specifications of the EBR-II tests are also being used to support code validation efforts during SAM development. Preliminary SHRT-17 benchmark simulation results were presented in Ref. [1]. Major physics phenomena in the primary coolant loop during the protected-loss-of-flow transients were well captured in the SAM simulation. This paper presents the benchmark simulations of SHRT-45R and an unprotected loss of all heat rejection test, BOP-302R.

The SHRT-45R test was conducted to demonstrate the effectiveness of inherent feedback mechanisms in EBR-II to terminate the fission process. Starting from full power and flow, SHRT-45R was initiated by simultaneously tripping both the primary and intermediate-loop coolant pumps to simulate an unprotected loss-of-flow accident. Once the loss of flow transient began, forced convection flow continued while the pumps coasted down. After the pumps had stopped, the flow transitioned to natural circulation. The system then relied upon natural circulation to remove residual heat from the core. During the test, the plant protection system (PPS) was disabled to prevent a scram. Temperatures in the reactor quickly rose to high, but acceptable levels as the inherent reactivity feedbacks reduced the fission power. SHRT-45R demonstrated that natural phenomena such as thermal expansion of reactor materials could be effective in protecting the reactor against potentially adverse consequences from unprotected loss-of-flow accidents.

The BOP, or balance of plant, tests were a series of tests performed during the SHRT testing program to investigate transients where the primary sodium pumps did not trip. A variety of different BOP tests were performed ranging from tests where the control rod insertion depth fluctuated to other tests where the intermediate sodium electromagnetic pump was oscillated at various frequencies. BOP-302R was one of two loss of heat sink tests where the intermediate sodium pump was tripped without scramming the control rods or tripping the primary pumps. This test was driven by increasing core inlet temperatures, which were a result of a diminished IHX heat rejection rate due to the lower intermediate sodium flow rates. BOP-302R was performed several hours after SHRT-45R and was initiated from full power and full flow.

IV. MODEL DESCRIPTIONS

An EBR-II model, similar to the SAS4A/SASSYS-1 model described in Ref. [10], was developed for the SHRT-45R and BOP-302R benchmark simulations.

IV.A. Core

The thermal-hydraulic performance of a reactor core is analyzed in SAM with a model consisting of a number of core channels. The channel model provides input to specify a single fuel pin and its associated coolant and structure. A single-pin channel represents the average pin

in an assembly, and assemblies with similar reactor physics and thermal-hydraulic characteristics are grouped together.

Five single-pin channel types were created for the driver, partial driver, dummy, reflector, and blanket assemblies. The SHRT-45R and BOP-302R core models use 12 channels based on one of these five channel types to represent all 637 subassemblies. The safety, experimental, and control subassemblies are not modeled with their own channel types but rather are grouped into other channels. The same core model was used for both SHRT-45R and BOP-302R tests. Table 1 and Figure 1 illustrate the channels in the EBR-II core model. Among them, six channels (with six different colors in Figure 1) represent: (1) the lumped fuel assembly groups of the driver fuel assemblies; (2) the high-flow driver fuel assemblies; (3) lumped channel for all dummy (K-type), partial driver (P-type), experimental, and control assemblies; (4) inner core reflector assemblies; (5) outer core reflector assemblies; and (6) blanket assemblies. Another six channels shown in red represent six individual assemblies with different types at locations 1A1, 2B1, 4C3, 6C4, 7A3, and 12E6. These subassemblies were modeled individually because they were among a subset of subassemblies whose outlet temperatures were measured. A 22-channel model is used in SAS4A/SASSYS-1, and the details can be found in Ref. [10].

Reactivity feedbacks are not modeled in these benchmark simulations as some important reactivity feedback mechanisms, such as the radial and axial core expansion, control rod drive line expansion, etc., can not yet be modeled in SAM. Instead, the reactor power histories from the tests are directly applied in the simulation of the transients. Although these reactivity feedback mechanisms can be modeled in SAS4A/SASSYS-1, the same assumptions were used in both simulations for consistent comparisons of the thermal-hydraulics responses of the system throughout the transients.

IV.B. Coolant System

Figure 2 illustrates the EBR-II primary system model used in the SAS4A/SASSYS-1 simulations. A similar model is used in the SAM simulations except that the minor flow leakage paths were not modeled. The two primary pumps draw sodium from the cold pool and feed the high- and low-pressure flow paths. Sodium flows through the high-pressure inlet piping (e.g. E14➔E15➔E16) and is discharged into the high-pressure inlet plenum before flowing up through the inner core channels. Sodium flowing through the low-pressure inlet piping (e.g. E17➔E18➔E19➔E20➔E21) is discharged into the low-pressure inlet plenum before flowing up through the outer core channels. The inner core channels represent the first seven rows of subassemblies and the outer core channels represent the remaining subassemblies in rows 8-16. At steady state, the mass flow rates through the inner core and outer core subassemblies are approximately 390 kg/s and 70 kg/s, respectively.

The inner and outer core channels both discharge into the outlet plenum, which mixes the discharged sodium before it enters the Z-Pipe. The Z-Pipe is a double-walled pipe that contains the auxiliary EM pump. Sodium leaving the Z-Pipe flows through the intermediate heat exchanger before discharging into the cold pool.

TABLE I. SAM lumped core channels

Channel number	Representations	Total Assembly number	Total Power (MW)	Total Flow (kg/s)
1	Average Driver	56	33.7	232
2	Average High Flow Driver	18	10.3	67.5
3	Lumped Channel, K+X+P+Control	28	8.66	77.3
4	Average Inner Reflector	20	0.278	3.32
5	Average Outer Reflector	180	0.855	11.2
6	Average Blanket	329	4.50	64.5
7	1A1, Half-Driver	1	0.332	3.81
8	2B1, K016	1	0.0177	0.685
9	4C3, Driver	1	0.692	4.86
10	6C4, Driver	1	0.598	3.71
11	7A3, Reflector	1	0.0149	0.165
12	12E6, Blanket	1	0.0268	0.163
Total		637	60.0	469

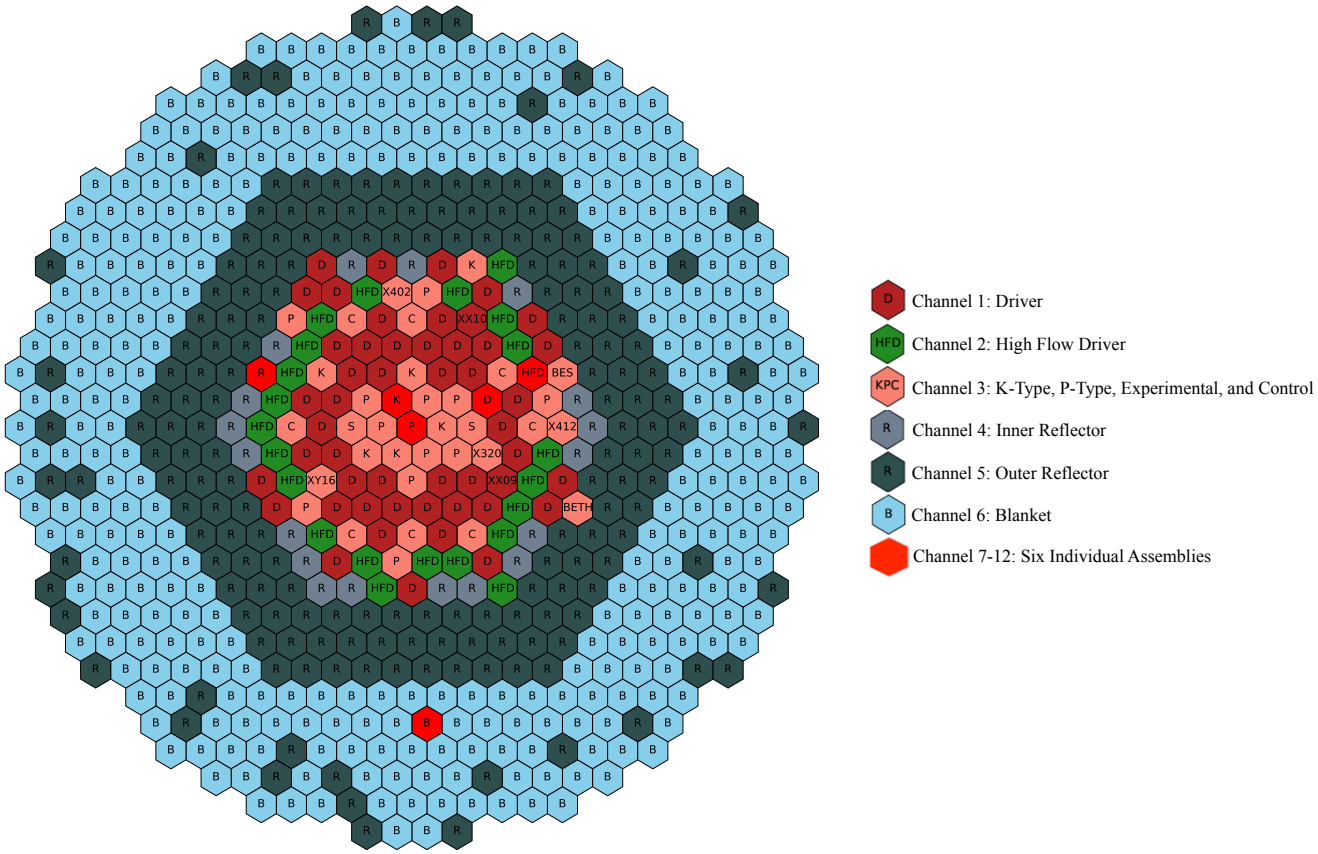

Figure 1. SAM Core Channel Model of EBR-II.

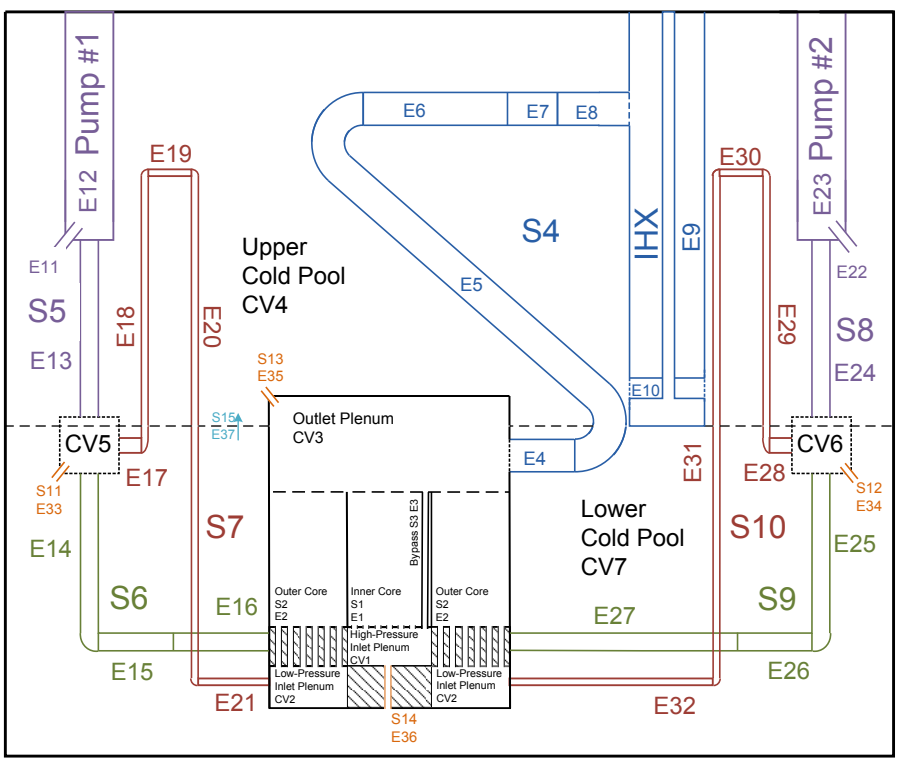

Figure 2. EBR-II Primary Sodium System Model.

IV.C. Boundary Conditions for Transient Modeling

As discussed above, the benchmark simulation focused on the thermal-hydraulics responses of the system throughout the transients in which the reactor power history was specified as input to the models for both SAM and SAS4A/SASSYS-1.

The complete intermediate loop was also not modeled in the benchmark tests. Instead, the IHX intermediate side inlet temperatures and mass flow rates are provided as boundary conditions. A simplified pump model is used in SAM for both tests in which the pump speed history during the tests are directly applied. Fig. 3 and 4 shows the IHX secondary conditions and the primary pump heads during the SHRT-45R test.

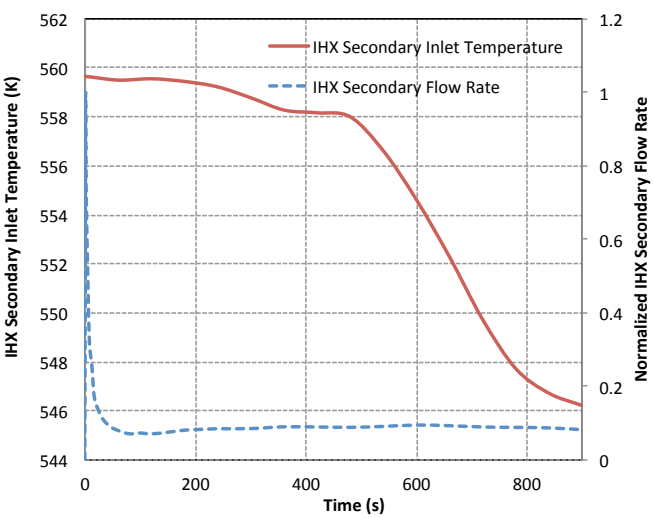

Figure 3. Boundary conditions of IHX secondary flow during SHRT-45R test.

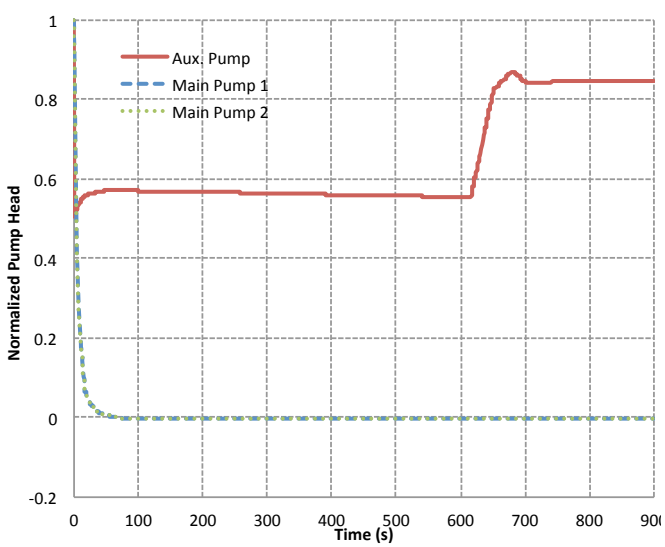

Figure 4. Normalized pump head history during SHRT-45R test

V. BENCHMARK RESULTS

V.A. SHRT-45R Results

Simulation results of the SHRT-45R test are shown in Figures 5-10. The reactor core power and the instantaneous heat removal rate of the IHX are shown in Figure 5. This transient is initiated by a complete loss of forced coolant flow in the primary and intermediate loops. The two primary pumps are designed with sufficient rotating inertia to maintain rotation until about 50 seconds after the start of the transient. This is followed by a transition to natural circulation. Immediately after the transient is initiated, the reactor temperature increases and the reactor power is slowly reduced due to various reactivity feedback mechanisms. After about 150 seconds, the reactor core power became lower than the IHX heat removal rate. This is expected since fair amounts of flow were remained for the intermediate heat transport system (IHTS) during SHRT-45R test. At the end of the 900-second test, the IHTS flow is still above 8% of the normal flow rate.

Figure 6 shows that the transition to natural circulation flow is very smooth. The transient response of the primary loop flow in the simulation is very close to that of the experiment and the SAS4A/SASSYS-1 simulation results, although the magnitudes are slightly different during the transition from forced flow to natural circulation flow. This is deemed successful considering the delicate coupling among the natural circulation flow, the friction and form losses, and the temperature distribution of the whole system.

Because the primary vessel is so large, the cold pool temperature does not change much during SHRT-45R. This leads to rather flat high-and low-pressure inlet plena temperature profiles. Both high- and low-pressure inlet plenum temperatures decrease several degrees during the test, likely due to over-cooling by the IHX through the later part of the transient.

The Z-Pipe inlet temperature is shown in Figure 7. The transient responses of the core outlet temperatures in the simulation are very similar to the experiment. The rapid flow decrease during the early part of the transient results in an increase of the core outlet and then the Z-Pipe inlet temperature. Core power decreases rapidly due to various reactivity feedback mechanisms. Once the natural circulation flow is fully established and because the IHX heat removal is higher than the core power, the core outlet and Z-Pipe inlet temperatures start dropping. The Z-Pipe inlet temperature rises faster in both SAM and SAS4A/SASSYS-1 simulations than the measured data because the upper plenum is modeled as a zero-dimensional volume. However, complex geometry and flow patterns existed in the EBR-II core outlet plenum. There is a delay as hotter sodium enters the volume, flows through or around the baffle plate, and enters the Z-Pipe, but it cannot be modeled in a 0-D volume. The Z-Pipe inlet temperature from the SAM simulation is slightly

over-predicted in the second half of the test, possibly due to the differences in the modeling of heat transfer between the upper plenum and the shield walls.

The IHX primary inlet temperature response during the transient is shown in Figure 8. Very large differences are found between both code predictions and the measurements while the two code predictions are very similar. Because the IHX inlet temperature thermocouple was installed inside the IHX along the outer surface of a tube, not at the inlet where higher flow mixing is expected, it is speculated that the IHX inlet thermocouple did not measure the average temperature of sodium leaving the Z-Pipe. The IHX inlet temperature is also significantly affected by the Z-Pipe heat loss due to the longer transit time in the Z-Pipe under low flow transient conditions. Figures 7 and 8 show that the IHX inlet temperature is significantly lower than the Z-Pipe inlet temperature during the transient, although it is only 1.5°C lower than the Z-Pipe inlet temperature under the steady state full flow conditions.

The core outlet temperature of driver fuel subassembly 6C4, highest power-to-flow ratio among all channels, is shown in Figure 9. The transient trends among the experiment and the two simulations are very similar, but the peak core outlet temperatures are different. It is suspected that there is a gap between the subassembly outlet and the temperature measurement location. Under low flow conditions, the mixing between the subassembly 6C4 and the adjacent low power subassemblies would reduce the core outlet temperature measurement in the test. The peak cladding temperatures from the SAM and SAS4A/SASSYS-1 simulations through the SHRT-45R test are shown in Figure 10. Almost identical results are found although different core channel groupings and different friction and form loss models are used. It can be confirmed that major fluid flow and heat transfer responses in the primary coolant loop during the unprotected loss-of-flow test can be captured by both the SAM and SAS4A/SASSYS-1 codes.

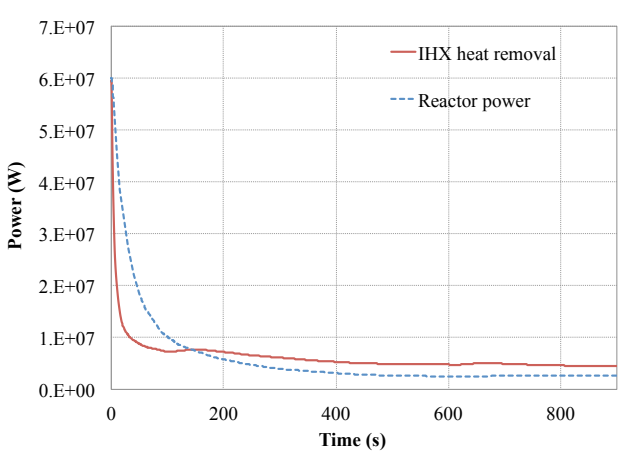

Figure 5. Reactor Power and IHX heat removal rate during SHRT-45R test

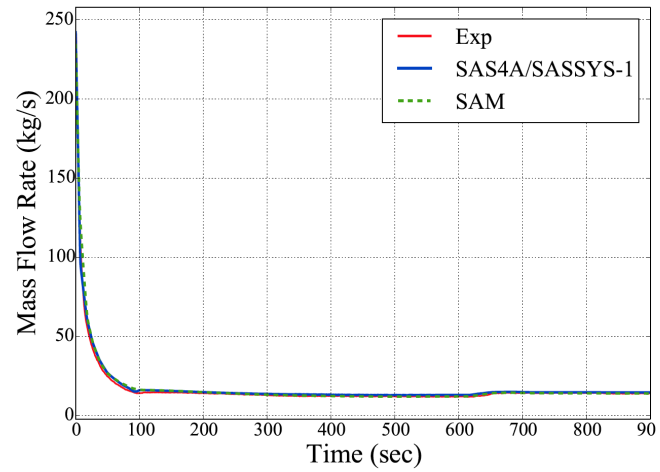

(a) Full range

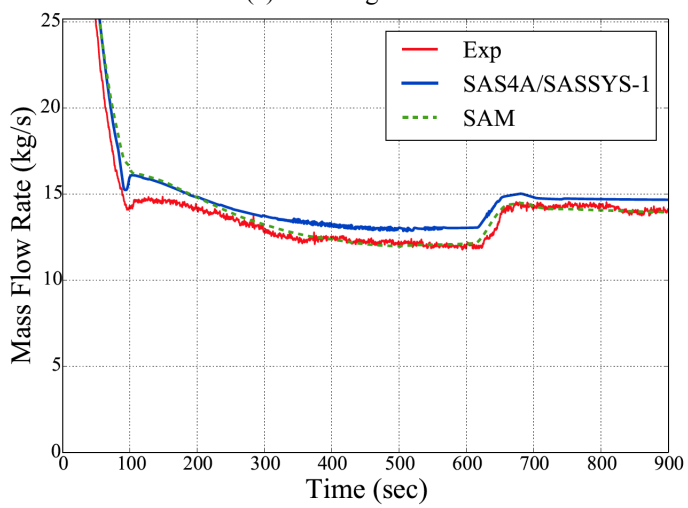

(b) Low range

Figure 6. Pump 2 mass flow rates during SHRT-45R test

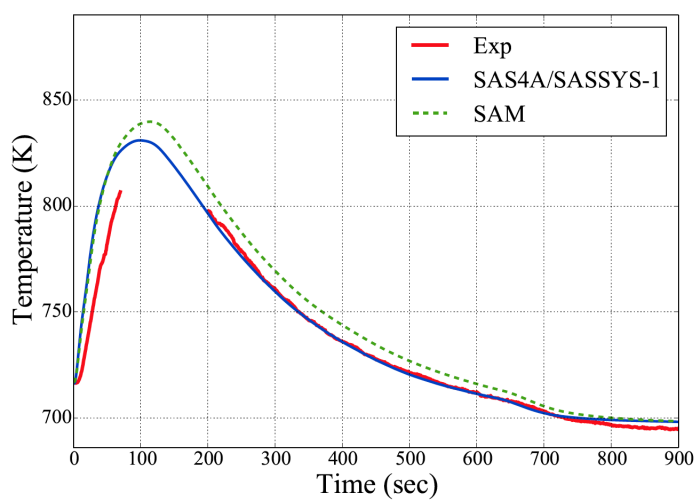

Figure 7. Z-Pipe inlet temperature during SHRT-45R test

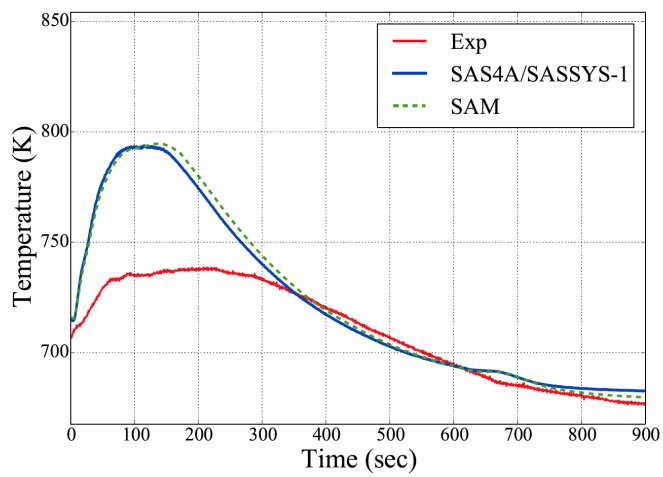

Figure 8. IHX primary inlet temperature during SHRT-45R test

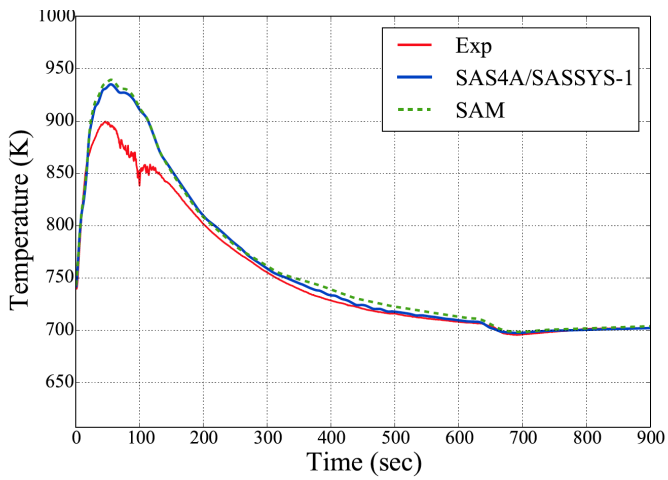

Figure 9. Subassembly 6C4 outlet temperature during SHRT-45R test

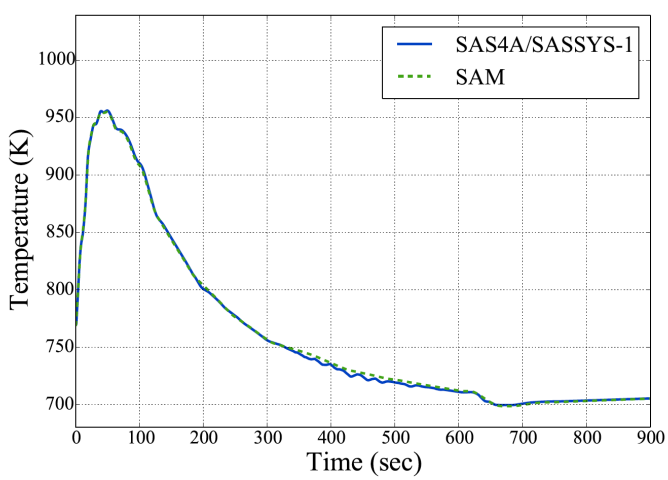

Figure 10. Peak in-core cladding temperature during SHRT-45R test

V.B. BOP-302R Results

BOP-302R was a loss of heat sink test where the intermediate sodium pump was tripped without scramming the control rods or tripping the primary pumps. This test was driven by increasing core inlet temperatures, which were a result of the diminished IHX heat rejection due to the lower intermediate sodium flow rates. Strong thermal stratification is expected in the primary vessel (cold pool), where the IHX outlet and the pump inlets are located in the upper part of the vessel. To correctly predict the core inlet temperature, the thermal stratification in the cold pool needs to be properly considered. This is accounted for in the SAM simulation with a two-volume pool model, in which the upper volume connects with the main primary pumps and the IHX, and the lower volume is stagnant but the mixing flow with the upper volume and the convective heat transfer with the immersed piping walls are considered. Similar modeling approaches were also applied in the SAS4A/SASSYS-1 model.

The StagnantVolume component is developed in SAM to model a stagnant volume with no connections to any 1-D fluid components, but allowing for heat transfer with other 0-D volumes or heat structures. For simplicity, it is assumed that the mass of the stagnant volume is unchanged. Only the energy conservation is needed for the stagnant volume component:

$$\frac{d(MH)}{dt} + \sum_{i=1}^{n} \dot{Q}_i = 0 \qquad (1)$$

In which, M: the total mass of the component; H: the average enthalpy of the component. t: time; n: the number of coupling heat transfer components; $\dot{Q}$: heat transfer with coupled heat structures or 0-D volumes; $\dot{Q} = \int h_{conv} \Delta T \, dA$ for heat transfer with heat structures; $\dot{Q} = \dot{m}_{mix} \Delta h$ for heat transfer with 0-D volumes, and $\dot{m}_{mix}$ is the mixing flow rate with the coupling 0-D volume. In the SAM BOP-302R simulation, the mixing flow between the upper and lower cold pool is assumed to be 50% of the primary core flow rate.

Simulation results of the BOP-302R test are shown in Figures 11-17. Very good agreement was found among the SAM and SAS simulations and the test results. It can be concluded that both the SAM and SAS codes can capture the major thermal-hydraulic responses in the primary coolant loop during the unprotected loss-of-heat-sink test.

The reactor core power and the instantaneous heat removal rate of IHX are shown in Figure 11. As discussed above, this transient is initiated by a complete loss of forced coolant flow in the intermediate loop, which resulted in a diminished IHX heat rejection rate. The reactor power is slowly reduced due to various reactivity feedback mechanisms. Throughout the transient, the reactor power is always higher than the IHX heat removal rate. For a short period, the IHX secondary side

temperature is higher than the primary side, which results in heat transfer from the intermediate loop to the primary loop.

SAM predictions of the plena temperatures during BOP-302R test are shown in Figure 12. The upper cold pool temperature increases rapidly at the beginning of the transient due to the loss-of-cooling in the IHX. As the primary loop coolant flow rate is largely unchanged throughout the transient, the core outlet plenum temperature drops with the decrease of the core power. As the IHX primary outlet temperature decreases and the continuous mixing between the upper and lower cold pool, the upper cold pool temperature decreases eventually after reaching a peak. The temperature responses in the high- and low-pressure core inlet plena are similar to the upper cold pool, and the temperature at the low-pressure inlet plenum is slightly lower due to the heat loss to the lower cold pool through the long piping. The lower cold pool temperature response is much slower compared to other volumes, as it does not directly participate in the primary coolant flow loop. Eventually all plena temperatures became very close to each other as the lower cold pool was heated up.

The comparisons of high- and low-pressure inlet plena temperatures from the SAM and SAS simulations and the test results are shown in Figure 13 and Figure 14. Very good agreement was achieved for both the initial heat up rates and the later pseudo-equilibrium states. It is demonstrated that the thermal stratification in the cold pool during the test can be modeled with a relatively simple multiple 0-D volume model. Note that the mixing flow rates between 0-D volumes are crucial to accurately model the heat transfer between 0-D volumes, and the mixing flow rates can be derived from RANS-based CFD simulations of the system at several different primary loop flow rates.

The Z-Pipe inlet and IHX primary inlet temperature responses are shown in Figure 15 and Figure 16. As the primary loop coolant flow rate is largely unchanged at full flow, the coolant temperature rise across the reactor core is very small. The core outlet temperature continues dropping as the reactor power decreases. The Z-Pipe inlet and IHX primary inlet temperature responses follow the same response. This is expected because the heat loss through the Z-Pipe walls is negligible during high flow conditions. Very good agreement was found among the two code simulations and the test results.

The core outlet temperature of the driver fuel subassembly 6C4 is shown in Figure 17. The transient trends among the experiment and the two simulations are very similar, but the initial increase of core outlet temperature was not observed in the test results. It is suspected again that the mixing between the subassembly 6C4 and the adjacent low power subassemblies reduced its outlet temperature measurement in the test. Very similar results are found between the SAM and SAS simulations.

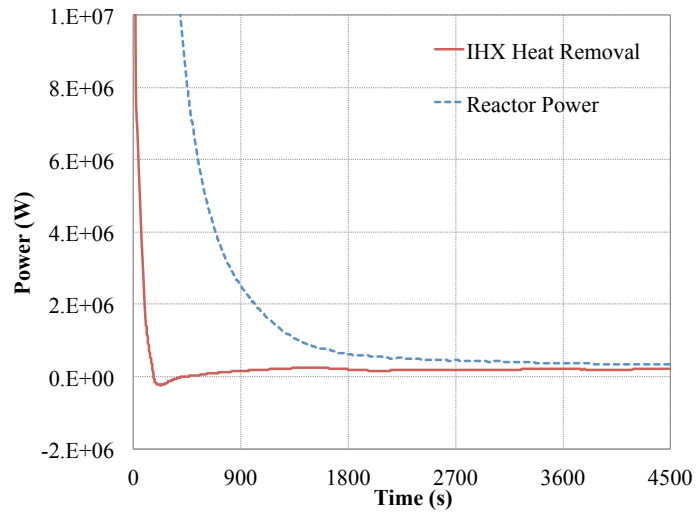

Figure 11. Reactor power and IHX heat removal rate during BOP-302R test

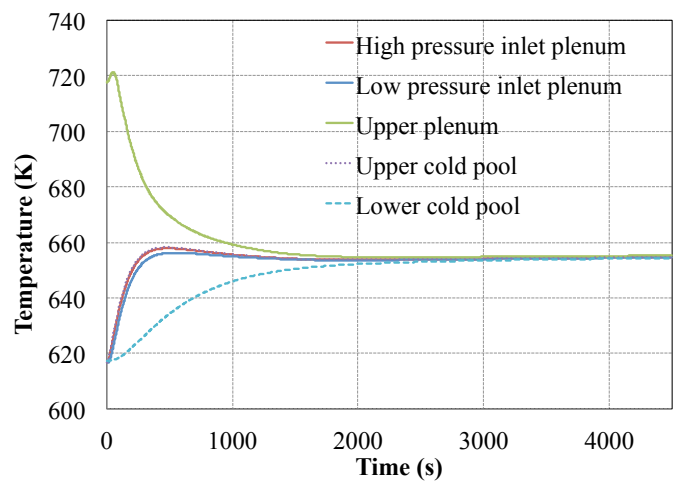

Figure 12. SAM predictions of plena temperatures during BOP-302R test

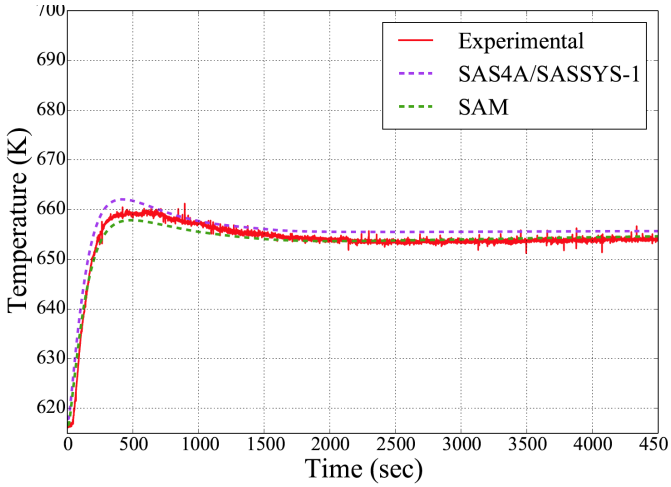

Figure 13. High-pressure inlet plenum temperature during BOP-302R test

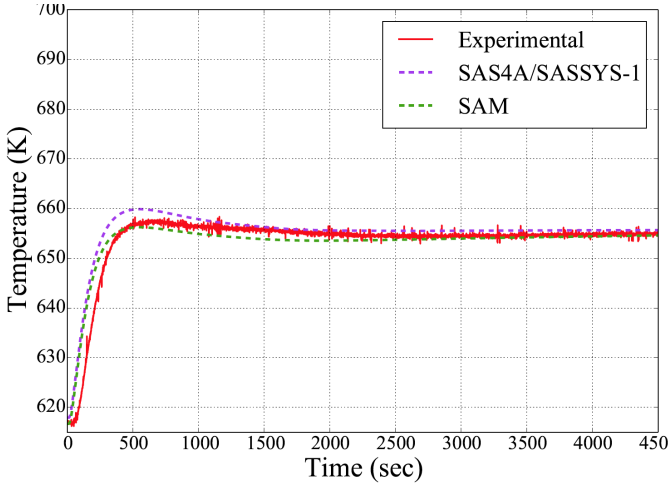

Figure 14. Low-pressure inlet plenum temperature during BOP-302R test

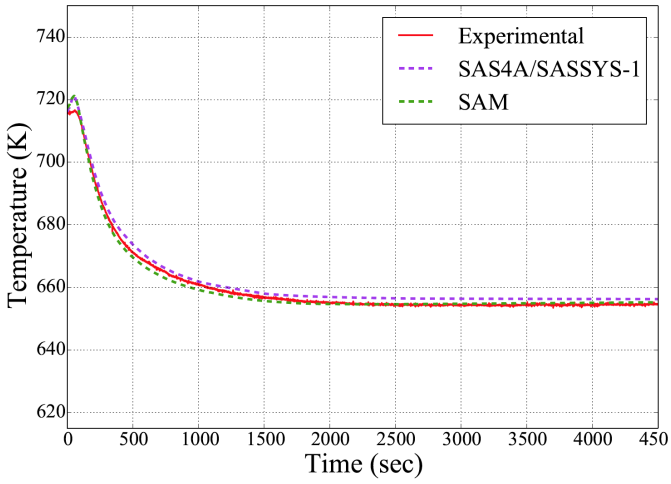

Figure 15. Z-Pipe inlet temperature during BOP-302R test

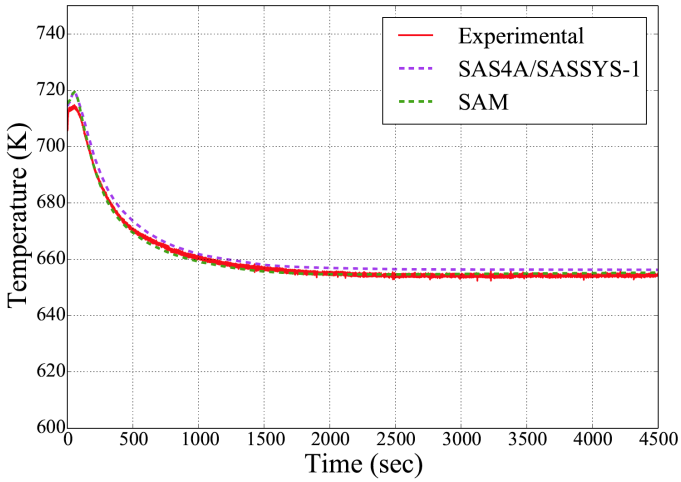

Figure 16. IHX primary inlet temperature during BOP-302R test

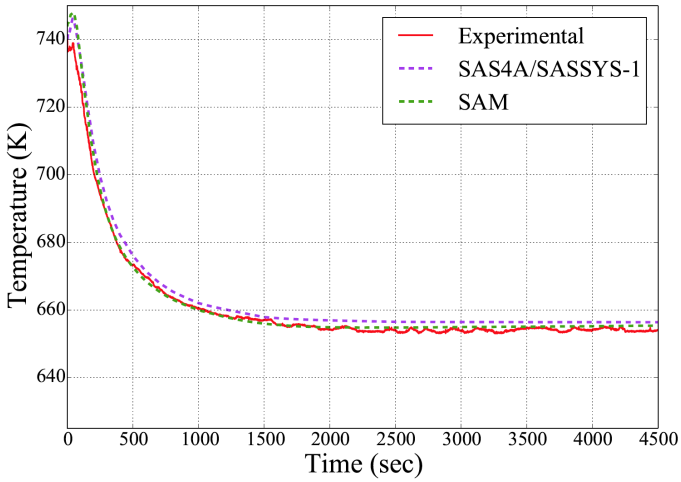

Figure 17. Subassembly 6C4 outlet temperature during BOP-302R test

VI. CONCLUSIONS

An advanced system analysis tool, SAM, is under development at Argonne National Laboratory for fast-running, improved-fidelity, whole-plant transient analyses. Validation activities are being conducted to assure the performance and validity of the SAM code. The benchmark simulations of two EBR-II tests, unprotected loss of forced cooling flow test (SHRT-45R) and unprotected loss of heat rejection test (BOP-302R) have been successfully performed.

The benchmark simulations focused on the thermal-hydraulics responses of the system throughout the transients in which the reactor power history was specified in both the SAM and SAS4A/SASSYS-1 models. Very good agreement was found among the two code simulations and the test results for both tests. For the SHRT-45R test, the transient response of the primary loop flow in the SAM simulation agreed very well with

the experiment during the whole transient, which went through the forced-flow during the pump coast-down, transition flow, and the natural circulation flow regimes. For the BOP-302R test, the high- and low-pressure inlet plena temperatures from SAM simulations agreed very well with the test for both the initial heat up rates and the later pseudo-equilibrium states, which demonstrated that the thermal stratification in the cold pool was correctly accounted for by the simple two-volume cold pool model. These results demonstrate that the SAM code can capture the major thermal-hydraulic responses in the primary coolant loop during SFR loss-of-flow and loss-of-heat-sink transients.

ACKNOWLEDGMENTS

This work is supported by U.S. Department of Energy Office of Nuclear Energy's Nuclear Energy Advanced Modeling and Simulation (NEAMS) and Advanced Reactor Technology (ART) programs. The submitted manuscript has been created by UChicago Argonne, LLC, Operator of Argonne National Laboratory ("Argonne") under contract No. DE-AC02-06CH11357 with the U.S. Department of Energy.

REFERENCES

1. R. Hu, T. H. Fanning, T. Sumner, Y. Yu, "Status Report on NEAMS System Analysis Module Development", ANL/NE-15/41, Argonne National Laboratory, December 2015.
2. D. Gaston, C. Newman, G. Hansen, and D. Lebrun-Grandi´e, "MOOSE: A parallel computational framework for coupled systems of nonlinear equations," *Nuclear Engineering and Design*, vol. 239, pp. 1768–1778 (2009).
3. B. S. Kirk, J. W. Peterson, R. H. Stogner, and G. F. Carey, "libMesh: A C++ Library for Parallel Adaptive Mesh Refinement/Coarsening Simulations," *Engineering with Computers*, 22(3-4): 237-254, (2006).
4. S. Balay, J. Brown, et al., PETSc Web page, http://www.mcs.anl.gov/petsc, 2015.
5. T. Sumner, T.Y.C. Wei, A. Moisseytsev, A. Mohamed, L.L. Briggs, unpublished information, Argonne National Laboratory (2012).
6. T. H. Fanning, ed., "The SAS4A/SASSYS-1 Safety Analysis Code System", Argonne National Laboratory, ANL/NE-12/4, January 31, 2012.
7. R. Hu, "An Advanced One-Dimensional Finite Element Model for Incompressible Thermally Expandable Flow", *Nuclear Technology*, Vol. 190, No. 3, 313-322, (2015).
8. R. Hu and Y. Yu, "Pseudo 3D Full-Core Conjugate Heat Transfer Modeling in Sodium Fast Reactors", *Proceedings of NURETH-16*, Chicago IL, USA, August 30-September 3, 2015.
9. L. L. Briggs, *et al.*, "EBR-II Passive Safety Demonstration Tests Benchmark Analyses - Phase 2", *Proceedings of NURETH-16*, Chicago IL, USA, August 30-September 3, 2015.
10. T. Sumner and A. Moisseytsev, "Simulations of the EBR-II Tests SHRT-17 and SHRT-45R", *Proceedings of NURETH-16*, Chicago IL, USA, August 30-September 3, 2015.